True Stress-Strain Behavior of Al-based Cast Automotive Alloy Under Different Ageing Conditions and the Effect of Trace Zr

Mashiur Rahman Shoummo[1], Akib Abdullah Khan[1], Mohammad Salim Kaiser[2*]

[1]Department of Mechanical Engineering, Bangladesh University of Engineering and Technology, Dhaka-1000, Bangladesh
[2]Directorate of Advisory, Extension and Research Services, Bangladesh University of Engineering and Technology, Dhaka-1000, Bangladesh
**Corresponding author:mskaiser@iat.buet.ac.bd*

Article history:
Received: 27 July 2022 / Received in revised form: 13 September 2022 / Accepted: 14 October 2022

ABSTRACT

A thorough investigation has been carried out on the Al-12Si-1Mg-1Cu-1Ni automotive alloy considering different properties, specially mechanical properties associated with true stress and true strain with Zr addition of trace amount. A commercially available piston is melted to produce the alloy, and trace amount of Zr is added to make another. The base alloy along with the Zr added alloy had been applied to homogenization, solution treatment, quenching, and ageing in order to get the age-hardening response. The alloys have been heat-treated at 25 ºC, 200 ºC, and 300 ºC, respectively, for four hours for attaining the under, peak and over-aged states, respectively. During ageing, Al_2Cu and Mg_2Si phases are formed in the aluminium matrix leading to peak-aged strength, which is reduced at over-aged state because of coarsening of precipitation and recrystallizing, shown by the tensile and hardness properties. When Zr is added to the alloy, Al_3Zr phases appear while casting and heat-treatment, resisting the drop of strength at over-aged state. It is visible in the stress-strain diagram that at over-aged conditions, the alloy with trace Zr shows improved strength and ductility. In the micrographs of Zr added alloy, finer distributed grains are visible through the grain refinement of Zr, which also prevents recrystallization at over-aged conditions. The homogeneity of the grains as a result of the Zr addition's microstructural change was further confirmed by fractography. It is clear that adding Zr to such alloys does not greatly increase their strength, but it does restrict the declining of strength by preventing the production of thermally stable Al_3Zr precipitates, which coarsens the resisting behavior of various intermetallics in the thermally damaged alloy.

Keywords: *Cast Al-alloy, fractured surface, grain refinement, heat-treatment, Zirconium.*

I. Introduction

Castability, weldability, machinability, wear resistance, and corrosion resistance are among the mechanical qualities of the 4xxx series aluminum alloys, which have been widely employed in vehicle parts [1]-[3]. The amount of alloying element Si is used depending on the needs of the structure as it will be light or heavy duty. The range of Si level is generally considered to be 5 to 23 wt%. The cast alloys of lower Si content consist of primary α-Al and Al–Si eutectic mixture. However, increasing Si percentages exhibit a coarse microstructure that leads to poor mechanical properties. Beyond the eutectic composition 12.6% wt. primary Si particles begin to develop the massive phase of star-shape block morphology which direct to further degradation in mechanical properties [4], [5]. In most cases, 12-13 wt.% Si is well thought out to get better performance considering all the features. Heat treatment is not possible with these alloys. Magnesium and copper are used

DOI: 10.17977/um016v6i22022p095

to give the product age-hardening properties [6], [7]. These alloys are used to make automotive components because of their excellent mechanical properties. Aluminium's best qualities are obtained through alloying additives and subsequent heat treatment operations [8], [9]. Major and minor elements, microstructure modifiers, and impurities are the four categories of alloying elements. In some alloys, the impurity elements may be majors, while in others, they may be minors [10]-[12]. Major elements like as Si, Cu, and Mg are commonly used. Minor elements Ni and Sn are also considered. Ti, Zr, Sc, B, Sr, Be, Mn, Cr are considered microstructure modifiers, while Fe and Zn are considered impurity elements. They alter the microstructures and mechanical characteristics of aluminum alloys. When Zr is added to aluminum alloys, it creates the Al_3Zr phase, which is much finer and more coherent with the matrix. It's a great way to make the dispersoid stronger. This type of dispersoid can reduce recrystallization, refine the microstructure, and raise the recrystallization temperature and strength of matrix alloys [13], [14].

There are just a few researches on the impact of zirconium on cast Al-Si alloys. It is well known that the mechanical properties of such age hardenable alloys provide the most benefit while they are at their peak age and that the strength of the qualities decreases as the hardening temperature rises. The goal of this research is to look at the impact of trace Zr on the mechanical properties of an Al-Si automotive alloy, as well as the influence of ageing.

II. Material and Methods

A. Preparation of the Alloys

The master alloy was made by melting aluminum pistons in a clay-graphite crucible. In a resistance-heating furnace with a proper flux cover, the melting process took place. The Al-12Si-1Mg-1Cu-1Ni base alloy and the Al-12Si-1Mg-1Cu-1Ni alloy with trace zirconium were then developed from two samples. Within an aluminium foil cover, 99.98% pure Zr powder was taken and then immersed into the master alloy during melting. Table 1 shows the chemical composition, which were determined using spectrochemical techniques.

Table 1. Chemical composition of both the alloys by wt.%

	Si	**Mg**	**Cu**	**Ni**	**Fe**	**Zr**	**Al**
Alloy 1	12.280	0.919	1.120	1.306	0.521	0.001	BAL.
Alloy 2	12.410	0.938	1.130	1.328	0.554	0.024	BAL.

B. Preparation of the Test Specimen

The temperature of the base alloy melt was always been kept at 750°C, with a 2% temperature variation tolerance. The cast iron metal mould, which measures 16 x 150 x 300 millimetres, was preheated to 200°C. Following the casting process, the cast alloy was homogenized in a muffle furnace at 400°C for 18 hours. Following that, it was air cooled to ease internal stresses. The homogenized alloys were then solutionized for 120 minutes at 530°C to generate a supersaturated single phase zone, which was then quenched with salt-ice-water. The solutionized alloys were aged for 240 minutes at temperatures of 25°C, 200°C, and 300°C. Normally, ageing was perfected at 200°C, but samples were aged at the other two temperatures to account for the under-aged and over-aged scenarios [15].

C. Working Instruments and Test Data Collection Methods

Tensile Test

Tensile testing was conducted out at room temperature. The test was carried out on an Instron testing machine, with a fixed cross head designed to maintain a constant strain rate of $10^{-3}s^{-1}$. The samples have been set up to perform the tests in accordance with ASTM specifications. The gauge length of the samples was 25 mm. Five tests were undertaken at each condition and the closest value of the average of the results is used to build the true stress-strain curve.

Hardness Test

The Automatic Turret Micro Vickers Hardness Tester, model HV-1000DT, was used to measure the micro hardness of the aged samples. For the Knoop hardness test, a 1 kg load was given to the indenter for 10 seconds. The sample size of 5x 16x 16 mm was considered for this microhardness measurement. On each polished surface created by the fine grade emery paper of the aged hardened samples, a minimum of 10 indentations are made at varied locations.

Impact Test

The heat-treatedspecimens utilized were standard 10 x 10 x 55 mm specimens with a 2 mm deep V-shaped notch at a 45° angle. The impact testing was carried out in accordance with ASTM guidelines. The impact resistance of five test pieces was evaluated for each test.

Microstructural Study

Heat-treated alloy specimens were subjected to optical metallographic inspections following the tensile test. The specimens were etched with Keller's reagent after being polished with alumina. A Versamet-II microscope is then used to analyze the samples. A Jeol JSM-5200 scanning electron microscope was used to investigate the microstructure and fractography of fractured surfaces induced by tensile testing.

III. Results and Discussions

A. Interpretation of Tensile Tests

The true stress and true strain findings obtained from the tensile test at under-aged, peak-aged, and over-aged conditions are depicted in Figures 1, 2, and 3. The slopes of the graph of Alloy 1 decrease from the under-aged to the peak aged condition, as can be shown. The dislocation theory can explain this rise in strength. A precipitated particle acts as a barrier to dislocation motion. As a result of the obstruction, dislocation motion is slowed, and the slope lowers, with a corresponding increase in tensile strength. It is well recognized that at the peak aged condition this type of alloys attain the maximum amount of fine dispersoids precipitates as it strengthens the alloys. Significant differences in the slope of Alloy 2 cannot be seen in the under-aged condition, however due to grain refinement, morphological changes have occurred, resulting in a decrease in brittleness in the peak aged condition [16], [17]. Stress reliving of the cast alloys due to ageing also responsible for higher elongation. At the under-aged condition that is solutionizing state the maximum concentration of the elements remains in solid solution, so in this condition the alloys do not offer the additional strength.

The slope of the stress-strain curve of the alloys rises as it reached at over-aged circumstances. It is due to precipitation coarsening phenomenon into the alloys. The coarsening precipitate loses its inhibitory property to hinder dislocation migration as it becomes coarsen. The trace Zr Alloy 2, on the other hand, forms Al_3Zr trialuminide particles that are extremely resistant to coarsening and re-dissolution, cause a more uniform distribution of dislocations and pin grain boundaries even after peak aging, and undergo morphological changes that result in silicon precipitate modification. When compared to the base alloy, Alloy 1, the strength improves [18].

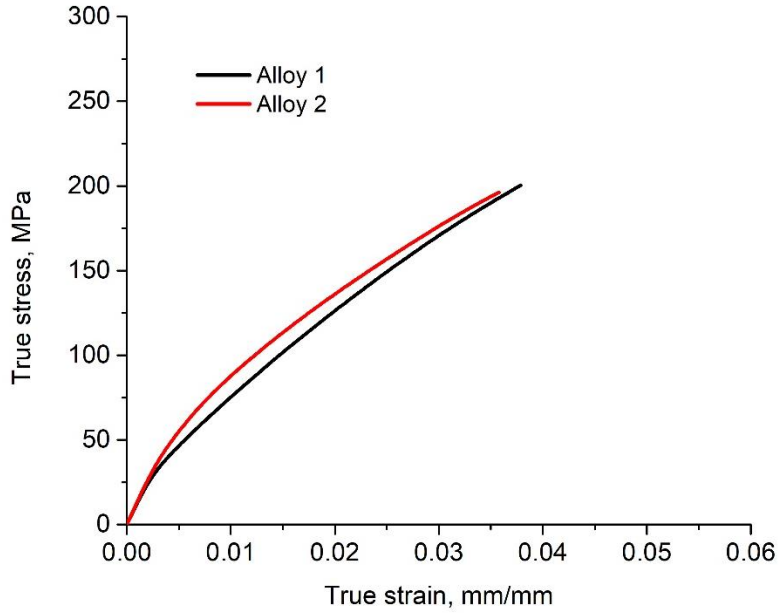

Fig. 1. True stress-true strain curves of the experimental alloys at under-aged condition.

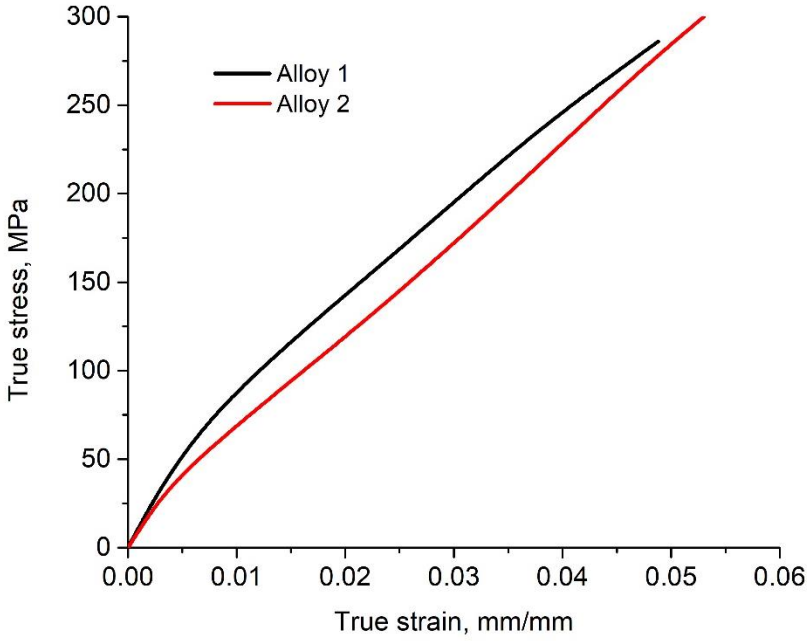

Fig. 2. True stress-true strain curves of the experimental alloys at peak-aged condition.

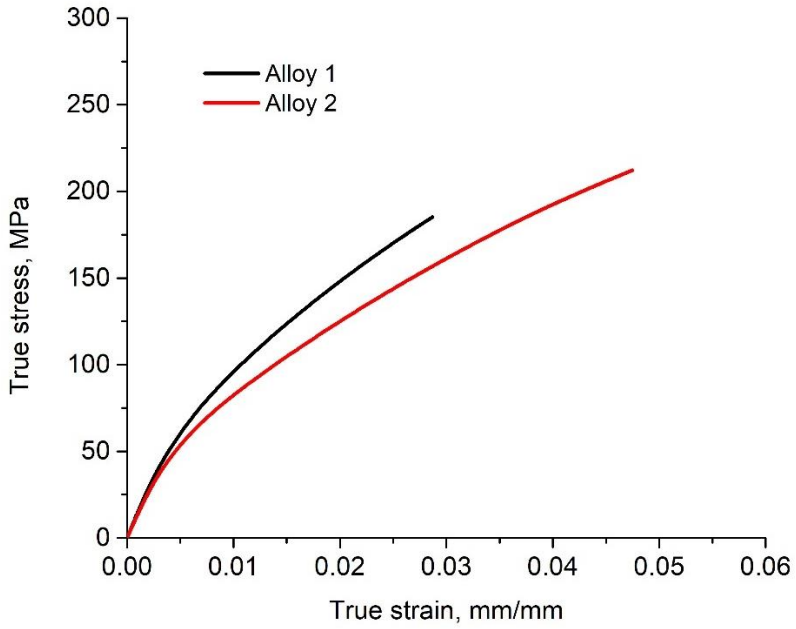

Fig. 3. True stress-true strain curves of the experimental alloys at over-aged condition

For better understanding the yield strength of both the alloys at under aged, peak aged and overaged condition is exposed the following bar chart in Figure 4. At under aged condition the yield strength is lower becase of alloying elements remain in solid solution. In this stage there is no additional benefit of Zr more over the yield strengthcompactdue to morphological change of brittle Si particles. At the peak aged condition, the yield strength improved due formation of different intermetallics as stated earlier but Zr added alloy shows healthier strength only for grain refining effects. The major benefit in terms of lower damagesof strength is displayed at over aged condition where Zr inhibit the precipitation coarsening and dislocation movement of the alloy [19].

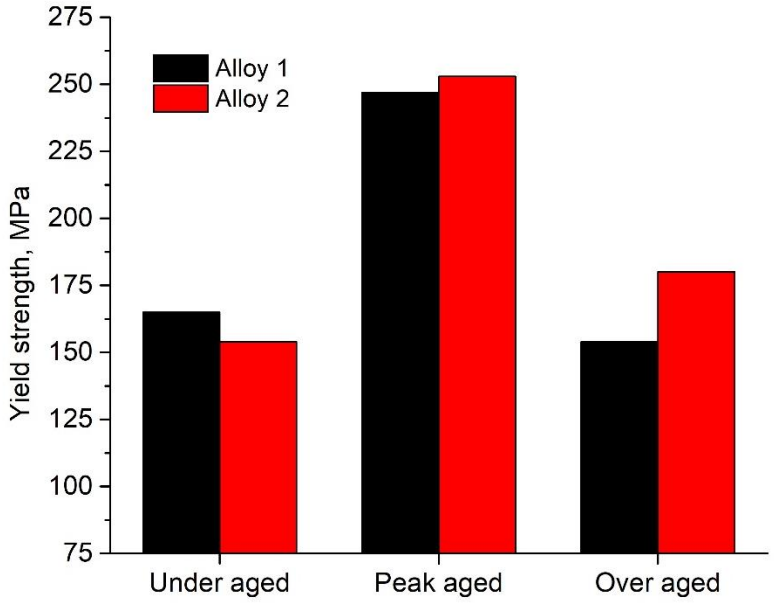

Fig. 4. Yield strength deviation of the experimental alloys at under aged, peak aged and over aged condition

B. Interpretation of Micro-Hardness Test

Similar patterns can be seen in the histogram provided in Figure 5 based on the findings of the micro-hardness test of the samples. The hardness of both alloys increases as the peak aged condition, however the rate of decline of hardness from peak aged to over-aged condition for Alloy 1 is greater than that of Alloy 2. The precipitation of both Al_2Cu and /or Al_2CuMg and Mg_2Si phases can explain this result. The presence of these intermetallic phases adds to a significant increase in matrix strength. The hardness drop in Alloy 1 is due to precipitation coarsening, as stated earlier in the over-aged condition. The Al_3Zr intermetallic, on the other hand, minimizes the softening effect of Alloy 2 under over-aged conditions [15], [19]. At the under aged condition the precipitates are not created into the alloys so lower the hardness values and the minimum difference of harness between the alloys.

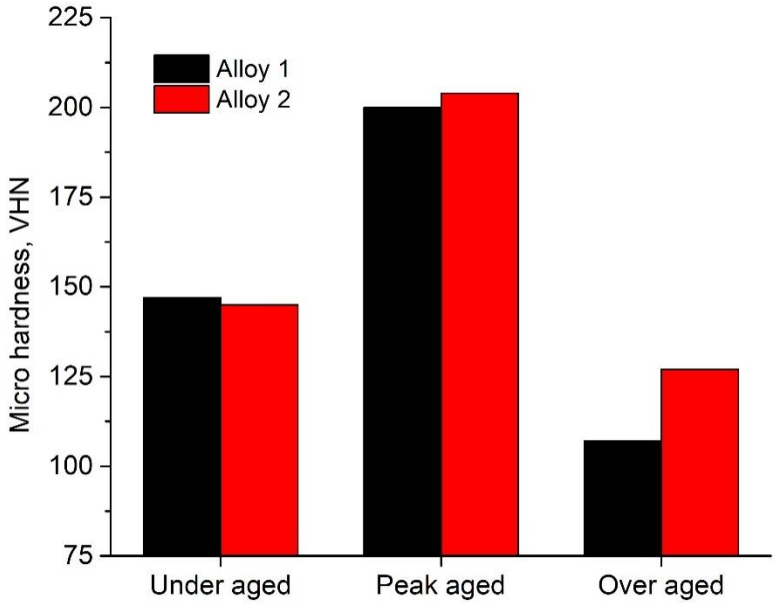

Fig. 5. Micro hardness variation of the experimental alloys at under aged, peak aged and over aged condition

C. Interpretation of Impact Test

Figure 6 depicts the impact toughness parameters of the experimental alloys at three different aged condition namely under-aged, peak-aged, and over-aged. It has been noticed that as precipitates get older, their impact energy declines. At the peak aged condition those are indication. The precipitation of both Al_2Cu and Mg_2Si phases resulted in a significant increase in matrix strength at the expense of ductility, resulting in this detection. Due to the reduced volume proportion of precipitates, the variation in impact strength of under-aged alloys is quite minor. The impact energy increases considerably from the peak-aged to over-aged condition due to precipitation and microstructural coarsening of the alloys. The figure also shows how trace added alloy as a microstructural alteration by Zr addition has a favorable impact on impact energy [19], [20]. It can be said in other words that the addition of Zr obviously reduced the Si particle size and changed its morphology resulting in reduced brittleness.

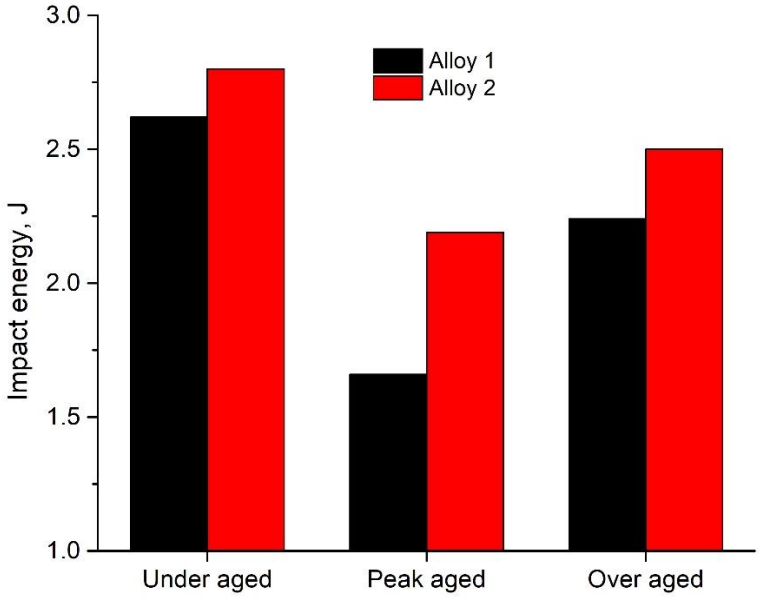

Fig. 6. Fracture toughness variation of the experimental alloys at under aged, peak aged and over aged condition

D. Interpretation of the Microstructural Study

Figure 7 shows the optical microstructure of base Alloy 1 and trace Zr added Alloy 2 at under aged, peak aged and over-aged conditions. Aluminumα-phase, eutectic silicon, and intermetallic compound particles make up the microstructures of these alloys. The microstructure of trace Zr added Alloy 2 reveals a finer grain than that of base Alloy 1 at solution treated state that is considered as under aged conditionsof the alloys (Figure 7a and 7b). Zr refines the grain structure of all the Al-alloys through the formation of Al_3Zr particles, at the same time acts as nuclei during solidification as previously indicated [13]. There is also evidence of different intermetallics uniformly distributed within the microstructure. When the alloys are aged at 200°C for 240 minutes to achieve the peak aged condition, there are different types of fine precipitates are form within the matrix. The common precipitates are produced during ageing of this type of Al-12Si-1Mg-1Cu-1Ni alloy such as Al_2Cu, Mg_2Si, Al_5FeSi, Al_8Mg_3FeS, Al_3CuNi, Al_3Ni etc. But all the precipitates do not take part for strengthening of the alloys. However, this type of optical microstructure cannot reveal the precipitates, whereas trace-added alloy reveals a grain structure that is quite thin (Figure7c and 7d). Both the alloys show relatively clear space of α-matrix becase most of the elements take part to form the precipitates. When the alloys are aged at 300°C for 240 minutes, that is the over aged condition the microstructure of the base Alloy 1 entirely recrystallized, revealing the equiaxed grains, but the microstructure of the trace added Alloy 2 partially recrystallized, revealing the grain (Figure7e and 7f). It is already stated earlier that during solification and ageing Zr form the numerous nanosized Al_3Zr precipitates which is fully coherent with the matrix. The precipitates create an effective barrier of dislocation motion and hinder the precipitation coarsening of the alloys. As a result, it can able to prevent the alloy from the process of recrystallization [21]-[23].

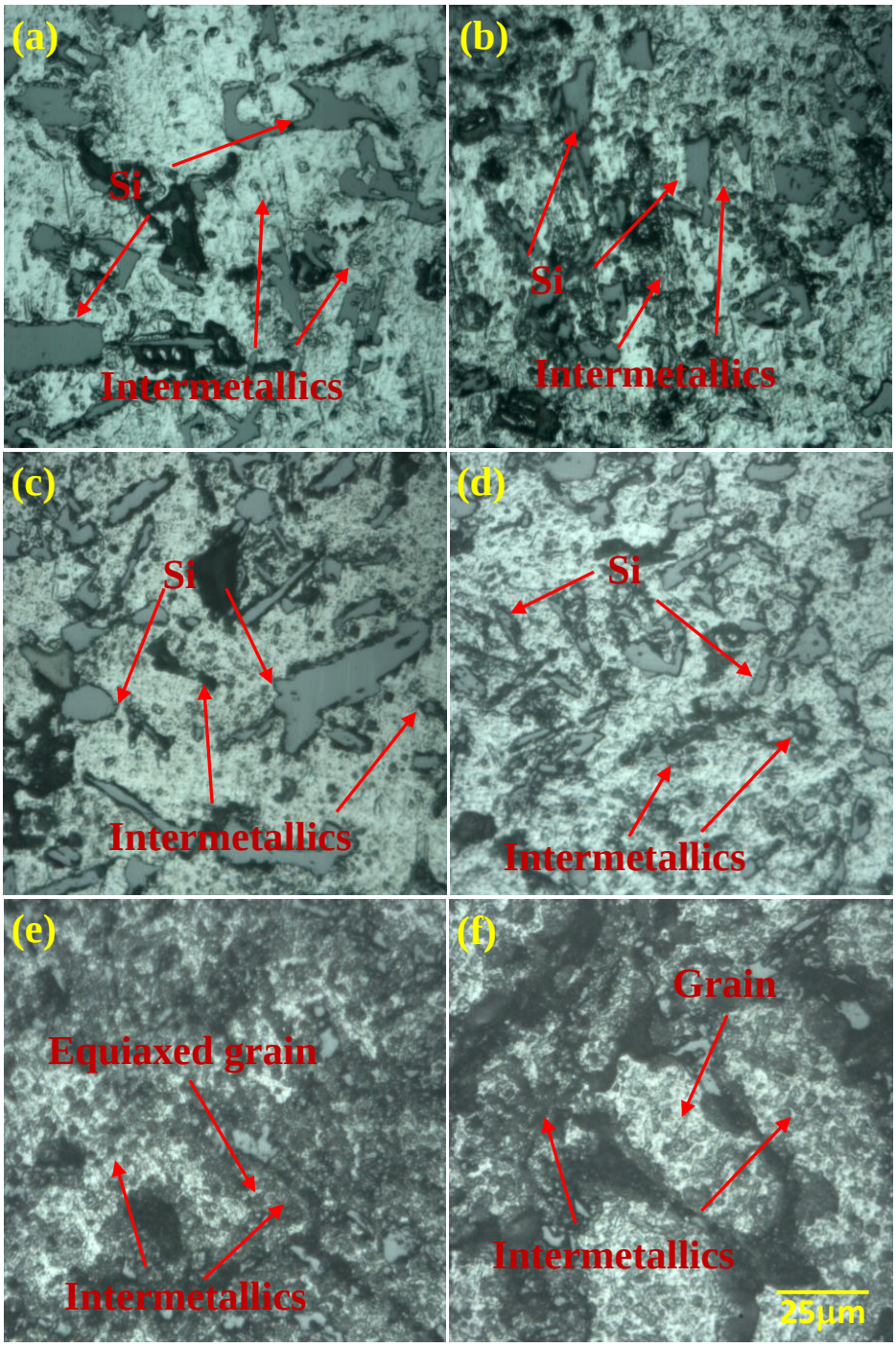

Fig. 7. Optical microstructure of solution treated Al–12Si–1Mg-1Cu automotive aged at 25°C for 240 minutes (under aged) (a) Alloy 1, (b) Alloy 2, aged at 200°C for 240 minutes (peak aged) (c) Alloy 1, (d) Alloy 2, aged at 300°C for 240 minutes (over aged) (e) Alloy 1 and (f) Alloy 2

A SEM images is used to confirm the findings as displayed in Figure 8. Both the alloys aged at 200°C for 240 minutes in peak aged condition, the effect of recrystallization is not very noticeable. Due to solution treatment and ageing the elements along with the intermetallic into the microstructure is well distributed. It is also visible that the silicon particles included plate like and niddle like morphology of different dimension relatively largein the base Alloy 1. In disparity, the particles turn into smallerwhen trace Zr is

supplementary to the Alloy 2. The low solubility along with the diffusivity properties of Zr creates the coherent particles which are more stable as a result refinementof Siparticlein the Al matrix [23], [24].

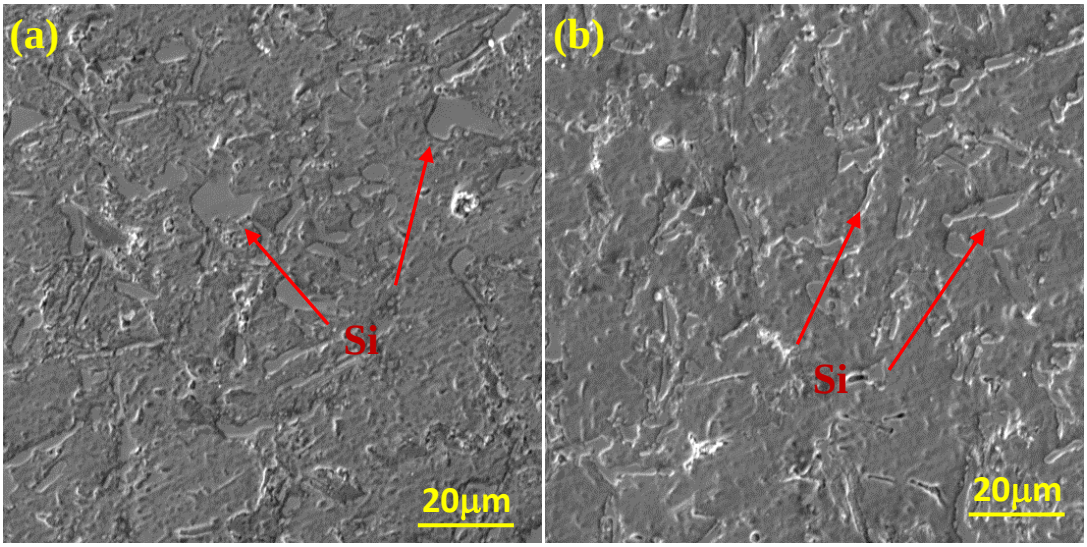

Fig. 8. SEM microstructure of Al–Si automotive alloy aged at 200°C for 240 minutes (a) Alloy 1 and (b) trace Zr added Alloy

Furthermore, once the alloys were fractured at the peak aged condition, SEM was performed as shown in Figure 9. Mode of brittle fracture clearly appears on the fracture surfaces of the base Alloy 1. The surface also consists of few dimples along with a feature of quasi-cleavage. With the addition of trace Zr the fracture surface of Alloy 2 displays the higher amount of the dimples. It also indicates the mixed mode of both ductility and brittle fractures. It is noticeable that the improvement of mechanical properties occurred through the grain refinement and eutectic Si modification. As a result, when Zr is added to an alloy, it improves its ductility [25]-[26].

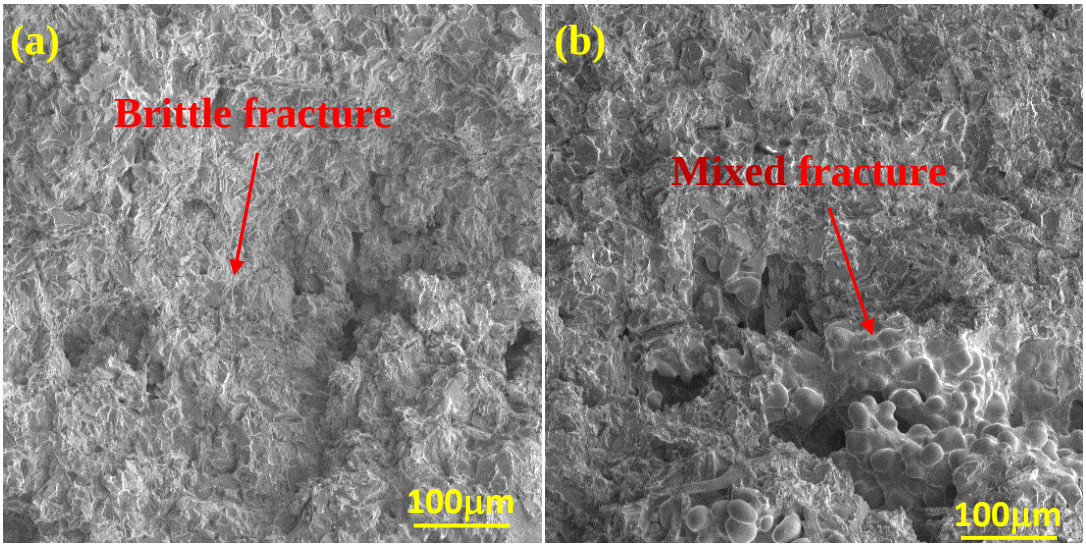

Fig. 9. SEM fractograph of Al–Si automotive alloy (a) Alloy 1 and (b) Alloy 2 aged at 200°C for 240 minutes and tensile tested at strain rate of $10^{-3}s^{-1}$

IV. Conclusion

After all the experimental interpretation it can be concluded that addition of Zr does not significantly improve the tensile strength of Al-Si Automotive alloy, but it slows down the rate of reduction in strength. The strength of the alloy decreases significantly in over aged condition due to coarsening of different intermetallic in order to reach in an equilibrium state. In contrast, the inclusion of trace zirconium holds the tensile strength at higher ageing temperatures due to the development of Al_3Zr precipitates, which build up the coarsening resistance and thermal stability of the alloy. Along with tensile strength the hardness also increases in the over aged condition due to the addition of Zr but this increase in strength and hardness is compensated at the expense of ductility which is evident from the impact test.

It can be understand from the fractography that relatively higher strength and hardness can be gained at peak aged condition at the expense of ductility, addition of trace Zr can relatively improve ductility which is evident from the fracture surface at peak aged condition. This happens due to morphological change of Zr added alloy.

Acknowledgement

This work is supported by DAERS office of Bangladesh University of Engineering and Technology, Dhaka. Thanks to Department of Glass and Ceramics Engineering for providing the laboratory facilities.

References

[1] H. Ye, “An overview of the development of Al-Si-Alloy based material for engine applications,” *Journal of Materials Engineering and Performance*,” vol. 12, no. 3, pp. 288–297, 2003, https://doi.org/10.1361/105994903770343132.

[2] M. Guo, M. Sun, J. Huang, and S. Pang, “A Comparative Study on the Microstructures and Mechanical Properties of Al-10Si-0.5Mg Alloys Prepared under Different Conditions,” Metals, vol. 12, no. 142, pp. 1–20, 2022, https://doi.org/10.3390/met12010142.

[3] M. A. Nur, A. A. Khan, S. D. Sharma and M. S. Kaiser, “Electrochemical corrosion performance of Si doped Al-based automotive alloy in 0.1 M NaCl solution” *Journal of Electrochemical Science and Engineering*, vol. 12, no. 3, pp. 565-576, 2022, https://doi.org/10.17977/um016v6i12022p009.

[4] M. Haghshenas, and J. Jamali, “Assessment of circumferential cracks in hypereutectic Al-Si clutch housings,” *Case Studies in Engineering Failure Analysis*, vol. 8, pp. 11–20, 2017, https://doi.org/10.1016/j.csefa.2016.11.003

[5] J. Abboud and J. Mazumder, “Developing of nano sized fibrous eutectic silicon in hypereutectic Al–Si alloy by laser remelting,” *Scientific Reports*, vol. 10, no. 1, pp. 1–18, 2020, https://doi.org/10.1038/s41598-020-69072-1.

[6] H. S. Abdo, A. H. Seikh, J. A. Mohammedand, and M. S. Soliman, “Alloying Elements Effects on Electrical Conductivity and Mechanical Properties of Newly

Fabricated Al Based Alloys Produced by Conventional Casting Process," *Materials*, vol. 14, no. 14, pp. 1–10. 2021, https://doi.org/10.3390/ma14143971.

[7] J. R. Davis, "*ASM Specialty Handbook: Aluminum and Aluminum alloys*," Cleveland OH, USA: ASM International, 1993.

[8] M. Gupta and S. Ling, "Microstructure and Mechanical Properties of Hypo / Hyper-Eutectic Al–Si Alloys Synthesized using a Near-net Shape Forming Technique," *Journal of Alloys and Compounds*, vol. 287, no. 1-2, pp. 284–294, 1999, https://doi.org/10.1016/S0925-8388(99)00062-6.

[9] L. Pedersen and L. Arnberg, "The Effect of Solution Heat Treatment and Quenching Rates on Mechanical Properties and Microstructure in AlSiMg Foundry Alloys," *Metallurgical and Materials Transactions A*, vol. 32A, no. 3, pp. 525–532, 2001, https://doi.org/10.1007/s11661-001-0069-y.

[10] M. N. E. Efzan, H. J. Kong and C. K. Kok, "Review: Effect of Alloying Element on Al-Si Alloys," *Advanced Materials Research*, vol. 845, pp. 355–359, 2013, https://doi.org/10.4028/www.scientific.net/amr.845.355.

[11] M. M. Hamasha, A. T. Mayyas, A. M. Hassan, and M. T. Hayajneh, "The Effect of Time, Percent of Copper and Nickel on Naturally Aged Al-CuNi," *Journal of Minerals & Materials Characterization & Engineering*, vol. 11, no. 2, pp. 117-131, 2012, https://doi.org/10.4236/jmmce.2012.112009.

[12] M. S. Kaiser, S. Sabbir, M. S. Kabir, M. R. Soummo and M. A. Nur, "Study of mechanical and wear behaviour of hyper-eutectic Al-Si automotive alloy through Fe, Ni and Cr addition," *Materials Research*, vol. 21, no. 4, pp. 1-9. 2018, https://doi.org/10.1590/1980-5373-mr-2017-1096.

[13] J. Zhang, D. Ding, W. Zhang, S. Kang, X. Xu, Y. Gao, G. Chen, W. Chen, X. You, "Effect of Zr Addition on Microstructure and Properties of Al−Mn−Si−Zn-Based Alloy," *Transactions of Nonferrous Metals Society of China*, vol. 24, no. 12, pp. 3872−3878, 2014, https://doi.org/10.1016/S1003-6326(14)63545-7.

[14] Y. Hideo, and B. Yoshio, "The Role of Zirconium to Improve Strength and Stress-Corrosion Resistance of Al−Zn−Mg and A−Zn−Mg−Cu Alloys," *Transactions of the Japan Institute of Metals*, vol. 23, no. 10, pp. 620−630, 1982, https://doi.org/10.2320/matertrans1960.23.620.

[15] M. S. Kaiser, "Efffect of solution treatment on the age hardening behaviour of Al-12Si-1Mg-1Cu piston alloy with trace Zr addition," *Journal of Casting and Materials Engineering*, vol. 2, no. 2, pp. 30–37, 2018, https://doi.org/10.7494/jcme.2018.2.2.30.

[16] S. K. Shaha, F. Czerwinski, D. L. Chen and W. Kasprzak, "Dislocation slip distance during compression of Al–Si–Cu–Mg alloy with additions of Ti–Zr–V," *Materials Science and Technology*, vol. 31, no. 1, pp. 63–72, 2015, https://doi.org/10.1179/1743284714Y.0000000606.

[17] L.Y. Pio, "Effect of T6 Heat Treatment on the Mechanical Properties of Gravity Die Cast A356 Aluminium Alloy," *Journal of Applied Sciences*, vol. 11, no. 11, pp. 2048–2052, 2011, https://doi.org/10.3923/jas.2011.2048.2052.

[18] J. H. Kim, J. H. Jeun, H. J. Chun, Y. R. Lee, J. T. Yoo, J. H. Yoon and H. S. Lee, "Effect of precipitates on mechanical properties of AA2195," *Journal of Alloys and*

Compounds, vol. 669, pp. 187–198, 2016, https://doi.org/10.1016/j.jallcom.2016.01.229.

[19] M. S. Kaiser, "Solution treatment effect on tensile, impact and fracture behaviour of trace Zr added Al-12Si-1Mg-1Cu piston Alloy," *Journal of the Institution of Engineers, India, Series D*, Vol. 99, No. 1, 2018, pp. 109–114, 2018, https://doi.org/10.1007/s40033-017-0140-5.

[20] A. M. A. Mohamed, E. Samuel, Y. Zedan, A. M. Samuel, H. W. Doty, and F. H. Samuel, "Intermetallics Formation during Solidification of Al-Si-Cu-Mg Cast Alloys," *Materials*, vol. 15, no. 1335, pp. 1–24, 2022, https://doi.org/10.3390/ma15041335.

[21] A. Ma, N. Saito, I. Shigematsu, K. Suzuki, M. Takagi, Y. Nishida, H. Iwata, and T. Imura, "Effect of Heat Treatment on Impact Toughness of Aluminum Silicon Eutectic Alloy Processed by Rotary-Die Equal-Channel Angular Pressing,"*Materials Transactions*, vol. 45, no. 2, pp. 399–402, 2004, https://doi.org/10.2320/matertrans.45.399.

[22] J. H. Sandoval, M. H. Abdelaziz, A. M. Samuel, H. W. Doty, and F. H. Samuel, "Effect of Dispersoids and Intermetallics on Hardening the Al-Si-Cu-Mg Cast Alloys, *Advances in Materials Science and Engineering*, vol. 2021, pp. 1–15, 2021, https://doi.org/10.1155/2021/9933168.

[23] Z. Yunxiang, Z. Haidong, Z. Lin, L. Changhi, and W. Hanqi, "Effect of Zr Contents on Mechanical Properties of Cast AlSi7Mg0.4 Alloys," *Chinese Journal of Materials Research*, vol. 35, no. 3, pp. 209–220, 2021, https://doi.org/10.11901/1005.3093.2020.228.

[24] H. Qian, D. Zhu, C. Hu and X. Jiang, "Effects of Zr Additive on Microstructure, MechanicalProperties, and Fractography of Al-Si Alloy," *Metals*, vol. 8, no. 124, pp. 1–10, 2018, https://doi.org/10.3390/met802012424

[25] S. I. Park, S. Z. Han, S. K. Choi and H. M. Lee, "Phase Equilibria of Al3(Ti, V, Zr) Intermetallic System," *Scripta mater*, vol. 34, no. 11, pp. 1697–1704, 1996, https://doi.org/10.1016/1359-6462(96)00049-8.

[26] A. A. Razin, D. S. Ahammed, M. A. Nur and M. S. Kaiser, "Role of Si on machined surfaces of Al-based automotive alloys under varying machining parameters," *Journal of Mechanical and Energy Engineering*, vol. 6(46), no. 1, pp. 43-52, 2022, https://doi.org/10.30464/jmee.2021.6.1.43